

# Ion–Molecule Reactions of Halocarbon Cations with Polycyclic Aromatic Hydrocarbons in a Quadrupole Ion Trap

## Part II—Applications to Environmental Analysis

Andrew A. Mosi, William R. Cullen and Guenter K. Eigendorf\*

Department of Chemistry, University of British Columbia, Vancouver, British Columbia, V6T 1Z1, Canada

Ion–molecule reactions between the cations  $\text{CH}_3\text{CHF}^+$  and  $\text{CH}_3\text{CF}_2^+$  generated from 1,1-difluoroethane and gas chromatographic eluents from a sediment extract containing polycyclic aromatic hydrocarbons (PAHs) were used to differentiate groups of PAH structural isomers. Formation of specific adducts led to characteristic mass spectra for the different isomers. Differences in the ion chromatograms for  $\text{M}^+$ ,  $\text{MH}^+$ ,  $[\text{M} + \text{CH}_3\text{CHF}]^+$ ,  $[\text{M} + \text{CH}_3\text{CHF} - \text{HF}]^+$ ,  $[\text{M} + \text{CH}_3\text{CF}_2]^+$ , and  $[\text{M} + \text{CH}_3\text{CF}_2 - \text{HF}]^+$  ( $\text{M} = \text{PAH molecule}$ ) allowed the resolution of co-eluting isomers. As the ratio of yields of adducts was not changed by methyl substitution, it was possible to differentiate and quantitate alkylated PAHs for which standards were not available. By performing a series of transformations between the ion chromatograms of the most characteristic adducts, information on individual isomer groups could be deconvoluted from complex clusters of isomers. This ion trap/chemical ionization technique displayed calibration curve parameters similar to those for electron ionization analysis and limits of detection of 170 pg in the sediment extract. © 1998 John Wiley & Sons, Ltd.

*J. Mass Spectrom.* 33, 250–263 (1998)

**KEYWORDS:** polycyclic aromatic hydrocarbons; isomer differentiation; ion–molecule reactions; halocarbon cations; environmental analysis

### INTRODUCTION

Previously we reported<sup>1</sup> that the use of certain halo-carbons,  $\text{C}_p\text{H}_m\text{X}_n$  ( $p = 1-2$ ,  $m = 1-4$ ,  $n = 2-3$ ,  $\text{X} = \text{Cl}$ ,  $\text{F}$ ) as chemical ionization (CI) reagents in an ion trap resulted in the formation of reactive ions  $\text{R}^+$  that formed adducts of the type  $[\text{M} + \text{R}]^+$  and/or  $[\text{M} + \text{R} - \text{HX}]^+$  with polycyclic aromatic hydrocarbon (PAH) standards ( $\text{M}$ ). Structural isomers of PAHs were distinguished based on differences in their adduct-forming behaviour. Using haloethanes, both of the above adduct types could be generated, whereas with halomethanes only  $[\text{M} + \text{R} - \text{HX}]^+$  was observed in significant amounts.

Hence the availability of two major PAH product ions from haloethanes makes the latter more useful reactants for isomer differentiation purposes compared with halomethanes. Among the haloethane reagents examined,<sup>1</sup> 1,1-difluoroethane provided the largest number of different adduct-forming reactive ions  $\text{R}^+$  ( $\text{R} = \text{CH}_3\text{CHF}$  and  $\text{CH}_3\text{CF}_2$ ). Consequently, this compound was used as a reagent for work outlined in this paper. Effects of instrumental parameters on the formation of reactive ions and adducts have been discussed previously.<sup>1</sup>

PAHs are a large class of compounds which are dispersed into the environment through both natural and anthropogenic sources.<sup>2</sup> Many PAHs have been identified as carcinogens, and often their toxicological properties are isomer dependent.<sup>3</sup> Furthermore, the presence and abundance of particular isomeric PAHs (parent or substituted) can provide information on their origin. For example, the ratio of different methylphenanthrene isomers can be used to differentiate between combustion or petrogenic sources.<sup>4</sup> However, gas chromatographic (GC) co-elution of 1-methylanthracene with 4- and 9-methylphenanthrene complicates the analysis. Consequently, isomer-specific analyses are important for both toxicological and environmental reasons, as reported previously.<sup>1</sup>

Using standard GC/mass spectrometric (MS) methodologies with electron ionization (EI), isomeric differentiation is not possible and co-eluting isomers or isomers for which standards are not readily available cannot be identified and are generally grouped together according to their molecular masses.<sup>5</sup> For example, methylfluoranthenes, methylpyrenes and benzofluorenes all give rise to identical mass spectra with molecular ions at  $m/z$  216.

The GC/MS method reported here using 1,1-difluoroethane (1,1-DFE) as chemical ionization reagent generates isomer-characteristic mass spectral signatures, thus permitting isomer differentiation. Simple arithmetic manipulation of selected ion chromatograms permitted the resolution of the profiles of closely eluting isomers.

\* Correspondence to: G. K. Eigendorf, Department of Chemistry, University of British Columbia, Vancouver, British Columbia, V6T 1Z1, Canada; eigen@chem.ubc.ca

## EXPERIMENTAL

### Materials

Pure standards of 1- and 2-methylanthracene, 2-methylphenanthrene, 3,6-dimethylphenanthrene, 9,10-dimethylanthracene and benzofluorene were purchased from Aldrich (Milwaukee, WI, USA) and 1-methylphenanthrene, 2-methylfluoranthene, 2-, 4- and 7-methylbenz[*a*]anthracene, 3,9- and 7,12-dimethylbenz[*a*]anthracene, 2-, 3-, 4- and 5-methylbenzo[*c*]phenanthrene, 1,12-dimethylbenzo[*c*]phenanthrene and 8-, 9- and 10-methylbenzo[*a*]pyrene were purchased from AccuStandards (New Haven, CT, USA). All solvents used were of HPLC grade (Fisher Scientific, Nepean, ON, Canada).

1,1-Difluoroethane (Aldrich) was introduced into the ion source from a lecture bottle equipped with a regulator via the chemical ionization gas inlet.

### Environmental samples

The contaminated sediment was obtained from a settling pond at the Alcan aluminum smelter in Kitimat, British Columbia, Canada, as described elsewhere.<sup>6</sup> The sediment was freeze-dried and a 5 g sample was extracted for 15 min with 40 ml of dichloromethane–acetone (5:1) using an Accelerated Solvent Extraction System (Dionex, Sunnyvale, CA, USA) operated at 125 °C and 2000 psi. A 1 ml aliquot, containing 10 mg of crude extract, was flushed through a column containing 5 g of silica gel. A 10 µl (= 100 µg of crude extract) portion of the extract was diluted to 1 ml with toluene and used for the GC/MS analysis.

### Apparatus

All experiments were performed on a Saturn 4D GC/MS ion trap system (Varian, Walnut Creek, CA, USA) equipped with a Wave-Board for the generation of user-defined wave forms for application to the ion trap electrodes.

Gas chromatography was performed using a DB5 capillary column (30 m × 0.25 mm i.d., 0.25 µm film thickness) from J & W, (Folsom, CA, USA), which was inserted directly into the ion trap through a transfer line heated to 280–290 °C.

### Procedure

Gas chromatography. Introduction of the samples was performed via splitless injection of 1 µl of sample at 290 °C. The GC column temperature program was initial temperature 90 °C for 0.1 min followed by a 6 °C min<sup>-1</sup> ramp to 280 °C, a hold at 280 °C for 1 min and then a 20 °C min<sup>-1</sup> ramp to 300 °C and a hold for 20 min. Helium was used as the mobile phase at a linear

velocity of 32 cm s<sup>-1</sup>, corresponding to a flow of ~1 ml min<sup>-1</sup> into the ion trap. The GC/MS transfer line was held at 280–290 °C, with the trap itself being at 250 °C.

**Ion trap.** Operational details of the ion trap under CI conditions have been discussed previously.<sup>1</sup> Unless specified otherwise, all experiments reported in this paper were performed under Automated Reaction Control (ARC) with a target value of 10 000. Other CI parameters employed were ionization storage level 25 *m/z*, reaction storage level 25 *m/z*, maximum ionization time 2500 µs and maximum reaction time 128 ms.<sup>1</sup>

### Data analysis

The mathematical transformations discussed in this work were performed on mass spectral files that were first converted into text files using a binary to ASCII converter (MS2TXT file converter, Unitech, Cincinnati, OH, USA). Text files were then imported into a spreadsheet for performing the required calculations.

## RESULTS AND DISCUSSION

### PAH homologous series in sediment extract

The four groups of PAH isomers which will be discussed in this work are shown in Fig. 1. Numbered positions correspond to sites of possible monoalkyl substitutions. The diluted sediment extract was analyzed using the GC/ion trap conditions described above. The resulting total ion chromatogram (TIC) is reproduced in Fig. 2 (regions 1–4). These four chromatograms represent the four retention time windows where the four groups of structural isomers shown in Fig. 1 elute. PAHs eluting in these four retention time (*t<sub>R</sub>*) slots are listed in Table 1, together with the relative abundance values of their adducts ( $M + 27 = [M + \text{CH}_3\text{CHF} - \text{HF}]$ ,  $M + 47 = [M + \text{CH}_3\text{CHF}]$ ,  $M + 45 = [M + \text{CH}_3\text{CF}_2 - \text{HF}]$ ,  $M + 65 = [M + \text{CH}_3\text{CF}_2]$ ). From these data it appears that the *m/z* 47 ( $\text{CH}_3\text{CHF}^+$ ) ion gives rise to more abundant adducts, making it more useful for isomer differentiation. However, although the *m/z* 65 ( $\text{CH}_3\text{CF}_2^+$ ) ion is less abundant it can still be of use, especially in cases where isobaric interferences in the environmental matrix obscure the *m/z* 47 adducts. The presence of *m/z* 65 is not detrimental to the analysis and therefore this ion was not removed. The homologous series described in each region as C0, C1 and C2 refer to the carbon substitution pattern on the PAH (C0 = unsubstituted parent compound, C1 = monomethyl substitution, C2 = dimethyl or monoethyl substitution). With increasing substitution pattern (C0 → C2) the number of possible isomers will increase, leading to a larger number of co-eluting species, thus complicating the chromatographic data. The relative concentration of PAHs decreases along the homologous series from C0 to C2; this is expected since the PAHs in this sample were formed at high tem-

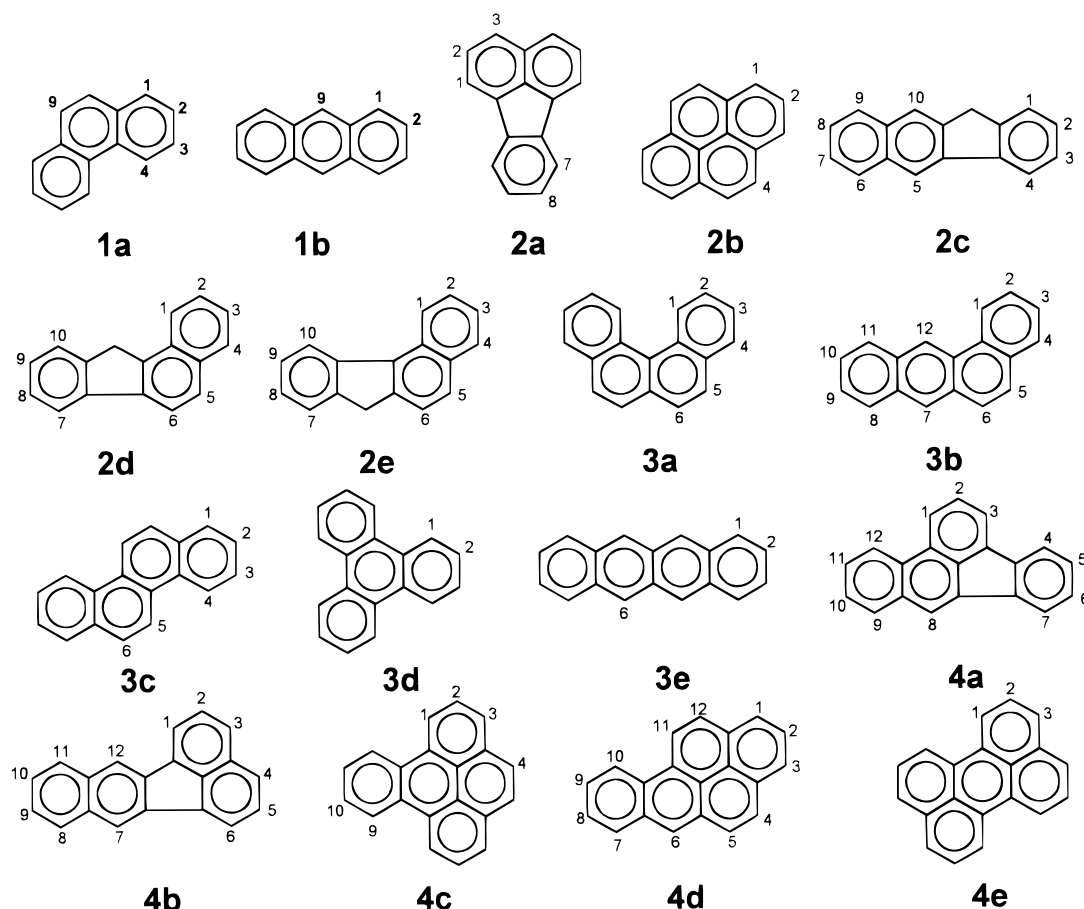


**Figure 1.** Structures of the PAHs analyzed: phenanthrene (**1a**), anthracene (**1b**), fluoranthene (**2a**), pyrene (**2b**), 11*H*-benzo[*b*]fluorene (**2c**), 11*H*-benzo[*a*]fluorene (**2d**), 11*H*-benzo[*c*]fluorene (**2e**), benzo[*c*]phenanthrene (**3a**), benz[*a*]anthracene (**3b**), chrysene (**3c**), triphenylene (**3d**), naphthacene (**3e**), benzo[*b*]fluoranthene (**4a**), benzo[*k*]fluoranthene (**4b**), benzo[*e*]pyrene (**4c**), benzo[*a*]pyrene (**4d**) and perylene (**4e**). Compounds are listed in their GC elution order.

peratures.<sup>4</sup> Alkyl PAHs above C<sub>2</sub> will not be discussed here since their concentration is near or below the detection limits in this sample.

#### Adduct formation and isomer differentiation

When a group of co-eluting substances produces a series of identical mass spectra they cannot be differentiated from each other. In order to differentiate co-eluting substances by mass spectrometry they must either yield unique characteristic spectra or, if they have ions at identical *m/z* values, the relative abundances of these ions have to be different for the co-eluting compounds.

The process of isomer differentiation relies on the formation of adducts in the gas phase leading to characteristic mass spectral fingerprints.<sup>1</sup> As shown previously, certain PAH structural isomers will react differently, leading to characteristic mass spectra under 1,1-DFE CI conditions. Although PAHs **1a** to **2b** are chromatographically separable, and therefore can be identified by a combination of their retention times and standard mass spectral information, the presence of characteristic mass spectral signatures for these compounds will still be useful for resolving them in samples containing co-eluting isobaric interferences. However, the method of

isomer differentiation discussed here will be of particular benefit to their alkyl-substituted analogues.

In the C<sub>1</sub> and C<sub>2</sub> PAH homologous series indicated in Fig. 2 there are many structural isomers which cannot be differentiated from each other owing either to the lack of analytical standards or, more importantly, because they co-elute.

For many alkyl PAHs, standards are not readily available, hence their adduct-forming behaviour has to be extrapolated from that of the unsubstituted more readily available parent analogues. To validate this extrapolation, a series of available methyl and dimethyl PAH standards were analyzed and compared with the corresponding unsubstituted PAHs using 1,1-DFE. The results in Table 2 indicate that the presence of methyl substituents in general results in a decrease of the relative amounts (with respect to  $M^+$ ) of both the protonated species  $MH^+$  and some of the adducts. In some instances (e.g. for 2-methylfluoranthene), the  $[M + R]$  adducts show a slight increase in relative abundance. As reported earlier,<sup>1</sup> it is the ratio of adduct formation of the different isomers that allows isomer differentiation and, although the addition of one or two methyl substituents does affect the amounts of adducts formed within one isomer group, it does not affect the relative adduct-forming behaviour between isomers. For example, the  $[M + 27]/[M + 47]$  relative abundance

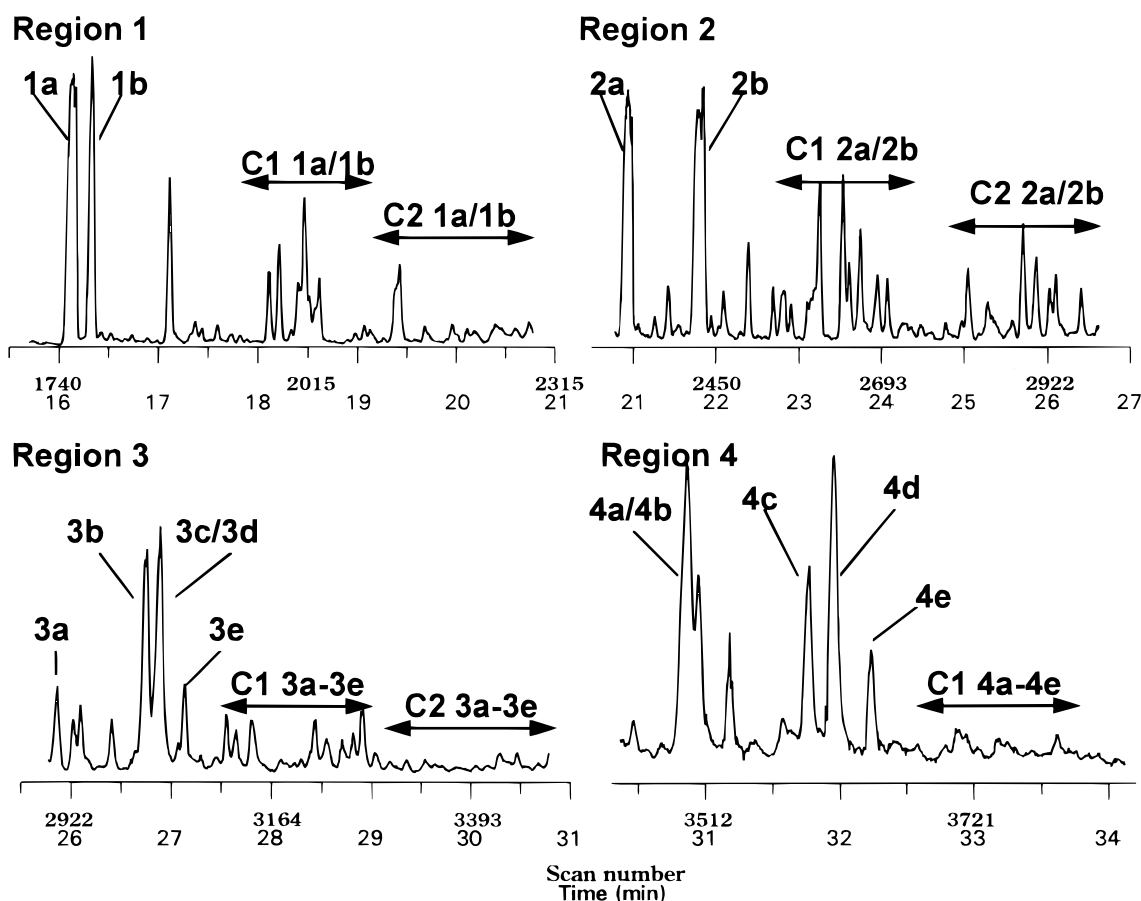


**Figure 2.** Total ion chromatogram of sediment extract obtained using 1,1-DFE CI showing the four isomer regions of interest in this work. C1 = monomethyl-PAHs, C2 = dimethyl/ethyl-PAHs.

ratio of C0, C1 and C2 phenanthrenes is an order of magnitude larger than for the C0, C1 and C2 anthracenes.

#### Data analysis methods for isomer differentiation

**Analysis of mass spectra.** Having subjected the sediment extract to a GC/1,1-DFE CI-MS analysis, the simplest way to search for presence of different structural PAH isomers in the complex chromatographic profile would be to examine the mass spectral data extracted from the TIC (Fig. 2). For example, in Fig. 3 the mass spectra from three positions along the C1 1a/1b homologue series (scans 181, 2015, 2037) and three positions along the C2 1a/1b homologous series (scans 2169, 2227, 2253) are listed. Mass spectra at scans 181 and 2015 clearly indicate the presence of a methylphenanthrene (C1-1a) and a methylanthracene (C1-1b), respectively, as indicated by the large amounts of  $m/z$  219 ( $M + 27$ ) in the former and the presence of  $m/z$  239 ( $M + 47$ ) in the latter (in addition to the lower abundance of  $M + 27$ ). The mass spectrum at scan 2037 contains smaller amounts of  $m/z$  219 than one would expect for a methylphenanthrene but more than is normal for a methylanthracene. Furthermore, the signal at  $m/z$  239 indicates the presence of a methylanthracene. Consequently, this spectrum demonstrates the presence of both methylanthracene and methylphenanthrene species

co-eluting together. Similarly, scans 2169 and 2227 are indicative of the presence of C2 phenanthrenes and anthracenes, respectively, while scan 2253 shows the presence of both isomers.

Although this type of analysis is useful to confirm (or exclude) the presence of a particular target compound, analysis of the extracted ion (mass) chromatograms for the major adduct ions will provide information on the elution profile for different isomers and also permit quantitation of various analytes.

**Analysis of mass chromatograms.** Analysis of the data from the sediment extract TIC is carried out by first plotting the mass chromatograms for  $M$ ,  $M + H$ ,  $M + 27$  and  $M + 47$  in the four different regions of the TIC. These ions generally display the largest differences between isomers. From these it is in some cases easy to observe the differences in adduct formation for each set of isomers. In other cases, particularly for the methylated analogues, the differences are more difficult to see. We have found that a simple transformation, for example  $[(M + 47) - (M + 27)]$ , of the mass chromatograms can enhance differences in the ion chromatograms, thus facilitating detection of the different isomers in the mass chromatograms. To illustrate this method, the mass chromatograms and "transformation chromatogram" (TCH) for the unsubstituted (C0) isomer pairs 1a/1b and 2a/2b are shown in Fig. 4. This transformation enables the 1b and 2b signals to plot positively whereas the 1a and 2a signals plot negatively.

Table 1. 1,1-DFE CI mass spectral data for selected PAH isomers from the settling pond extract

Region	PAH	$M_r$	Scan No.	$t_R$ (min) <sup>a</sup>	M	M + 1	Relative abundance (%)			
							R = CH <sub>3</sub> CHF <sup>+</sup>		R = CH <sub>3</sub> CF <sub>2</sub> <sup>+</sup>	
							M + R - HF M + 27	M + R M + 47	M + R - HF M + 45	M + R M + 65
1	C0 1a	178	1740	16.1	38	100	68	<1	10	3
	C0 1b	178	1763	16.3	100	45	13	12	<1	6
	C1 1a	192	1993	18.2	53	100	47	3	10	6
	C1 1b	192	2015	18.4	100	42	7	12	<1	7
	C2 1a	206	2169	19.7	70	100	50	4	7	4
	C2 1b	206	2227	20.2	100	54	10	13	2	5
2	C0 2a	202	2315	20.9	42	100	83	4	11	7
	C0 2b	202	2423	21.8	100	45	15	17	4	14
	2c, 2d, 2e	216	2630		100	84	36	23	7	17
	C1 2a	216	2543	22.8	63	100	58	7	8	8
	C1 2b	216	2681	23.9	100	41	10	20	1	9
	C2 2a	230	2780	24.8	26	100	46	7	6	6
3	C2 2b	230	2841	25.3	100	95	24	22	4	9
	C0 3a	228	2910	25.9	95	100	50	4	10	10
	C0 3b	228	3015	26.7	100	56	15	30	1	11
	C0 3c	228	3020–3030	26.9	98	100	50	11	6	16
	C0 3d	228	3020–3030	26.9	42	100	16	10	2	13
	C0 3e	228	3060	27.1	100	30	4	17	3	7
4	C1 3a–3e	242	3100–3360	27.2–29.3						
	C2 3a–3e	256	3200–3500	28.3–31.6						
	C0 4a	252	3490–3500	30.8–31.7	2	100	60	25	11	30
	C0 4b	252	3490–3500	30.8–31.7	100	64	25	28	3	22
	C0 4c	252	3615	31.7	2	100	20	86	4	32
	C0 4d	252	3640	31.9	100	28	1	19	0	7
	C0 4e	252	3673	32.2	100	26	1	6	0	1
	C1 4a–4e	266	3600–4000	32.0–34.5						

<sup>a</sup>  $t_R$  refers to the chromatogram shown in Fig. 1.

This approach becomes particularly useful when applied to the methylated PAH analogues. For example, Fig. 5 shows the  $m/z$  192 (M),  $m/z$  193 (M + H),  $m/z$  219 (M + 27) and  $m/z$  239 (M + 47) mass chromatograms for the C1 isomer series, and Fig. 6 shows the  $m/z$  206 (M),  $m/z$  207 (M + H),  $m/z$  233 (M + 27) and  $m/z$  253 (M + 47) mass chromatograms for the C2 isomer series. The data represent the most characteristic ions for these two groups of isomers.

Notable differences can be observed between these four chromatograms, similar to those observed for the chromatograms in Fig. 4. The  $m/z$  219 chromatogram shows mainly the presence of methylphenanthrenes (C1-1a) since phenanthrenes produce much larger amounts of the M + 27 ion than anthracenes. Similarly, the  $m/z$  239 (M + 47) chromatogram emphasizes the elution profile for the methylanthracenes (C1-1b) since the phenanthrenes produce only small amounts of ions at this

Table 2. Effect of methyl substitution on adduct formation under 1,1-DFE CI conditions

Substance	M	M + 1	Relative abundance (%)				Relative abundance ratio	
			M + 27	M + 47	M + 45	M + 65	M + 27 M + 47	M + 45 M + 65
Phenanthrene	38	100	68	<1	10	3	68	3.3
1- + 2-Methylphenanthrene	40	100	50	<1	8	5	50	1.6
3,6-Dimethylphenanthrene	98	100	46	<1	6	2	46	3.0
Anthracene	100	45	13	12	<1	6	1.1	0.17
1-Methylanthracene	100	47	12	12	<1	5	1.0	0.20
2-Methylanthracene	100	43	8	13	<1	6	0.6	0.17
1,9-Dimethylanthracene	100	25	1	7	<1	2	0.1	0.50
Fluoranthene	42	100	83	4	11	7	21	1.6
2-Methylfluoranthene	52	100	62	7	2	9	9	0.2
Benz[a]anthracene	100	56	15	30	1	11	0.50	0.09
2-Methylbenz[a]anthracene	100	52	10	21	<1	7	0.48	0.14
4-Methylbenz[a]anthracene	100	47	7	30	1	8	0.23	0.13
7-Methylbenz[a]anthracene	100	48	4	23	<1	5	0.17	0.20
3,9 + 6,8-Dimethylbenz[a]anthracene	100	40	6	15	<1	4	0.40	0.25
7,12-Dimethylbenz[a]anthracene	100	29	1	8	<1	4	0.13	0.25

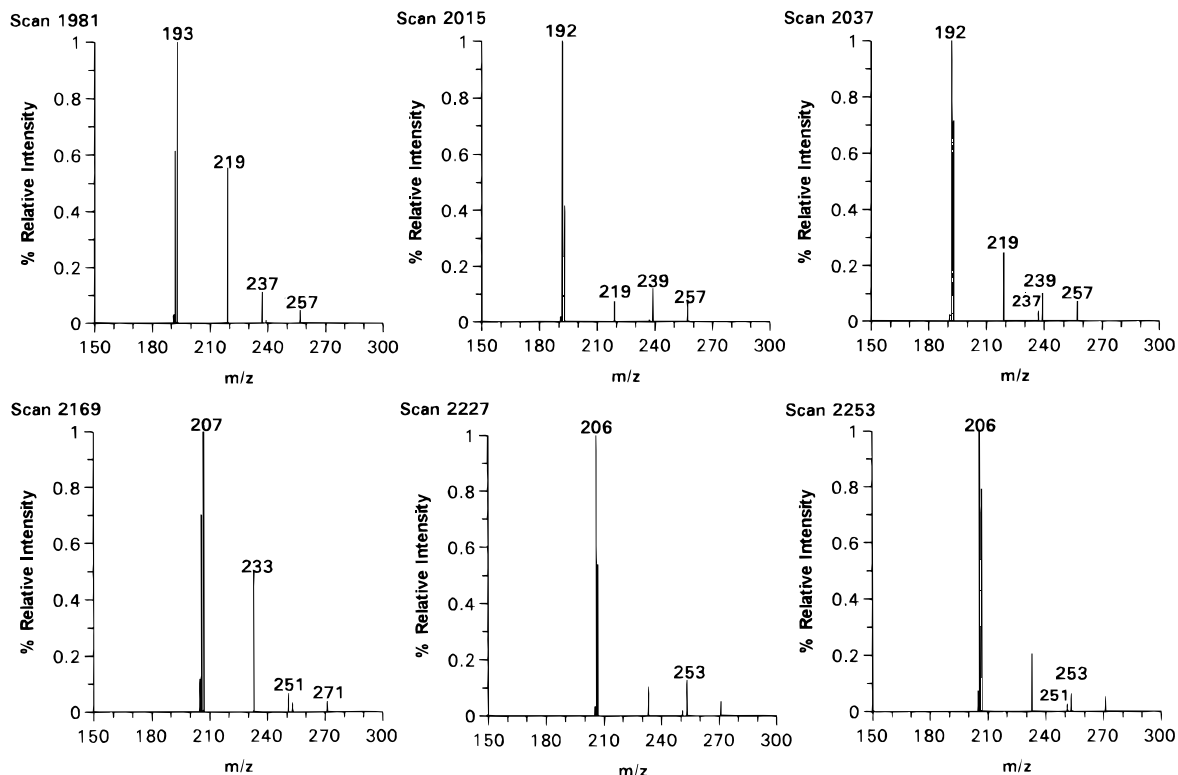


Figure 3. Mass spectra for C1 and C2 phenanthrenes and anthracenes present in the extract.

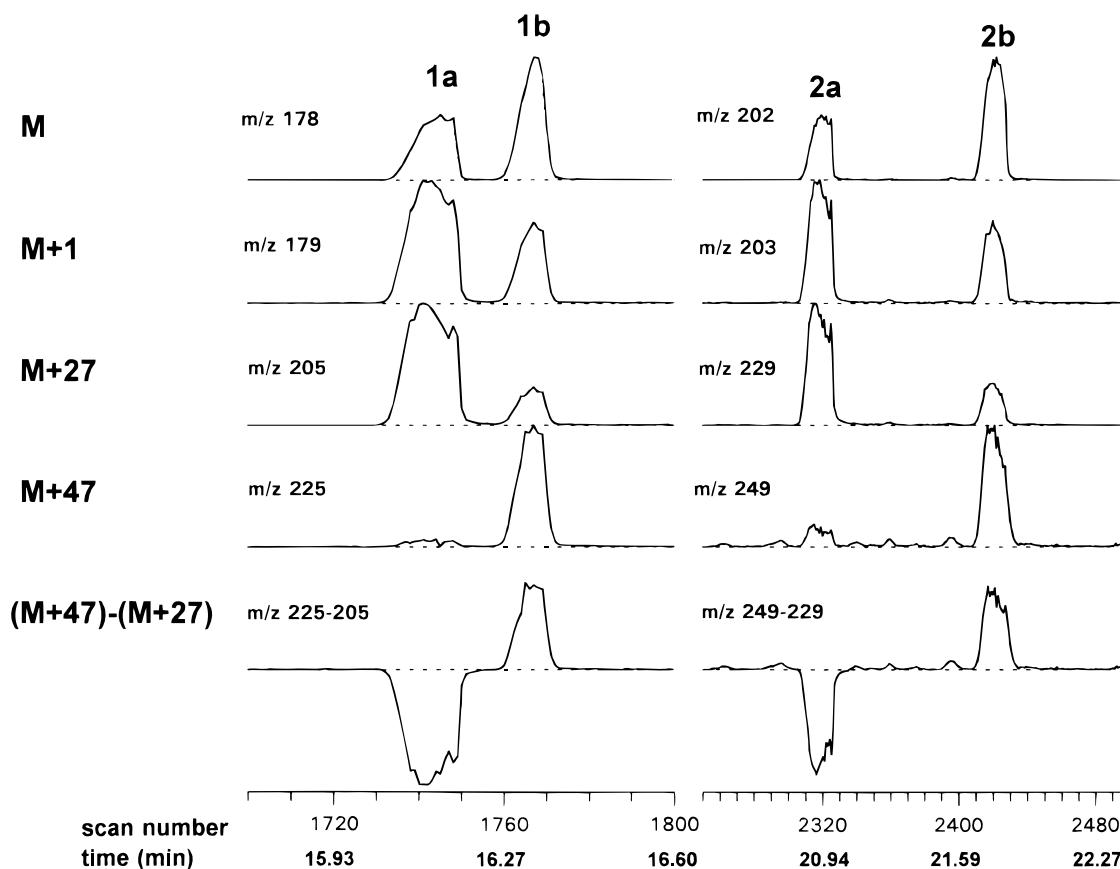
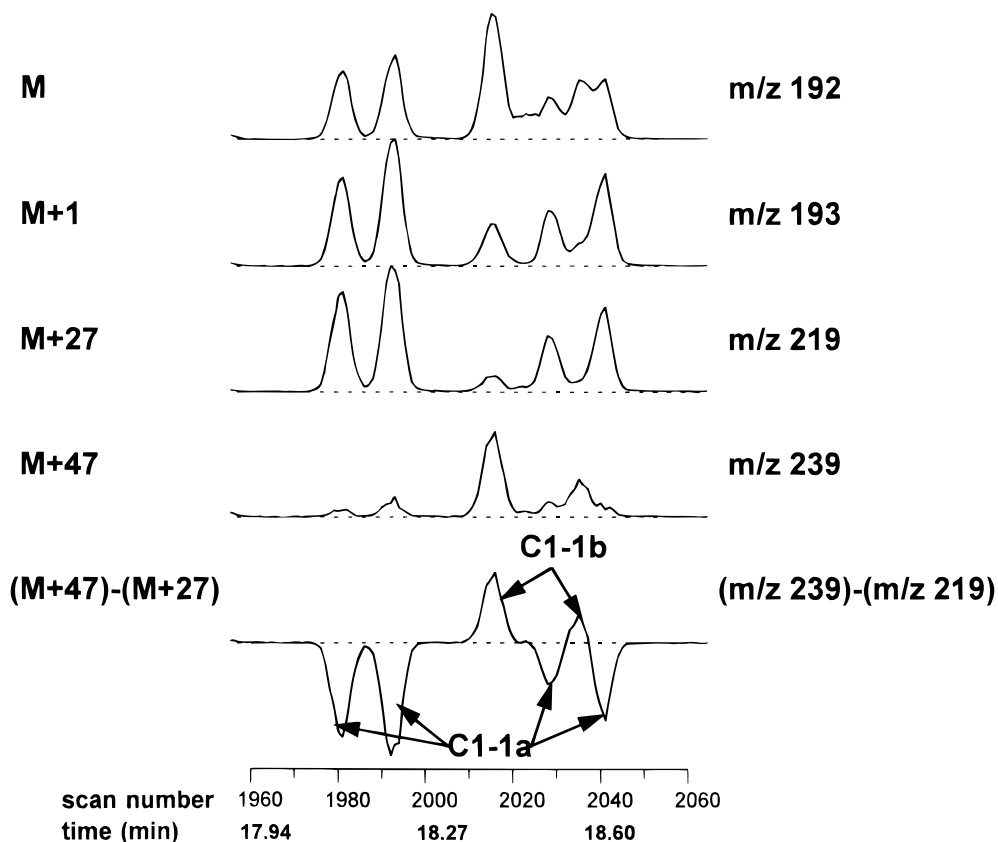
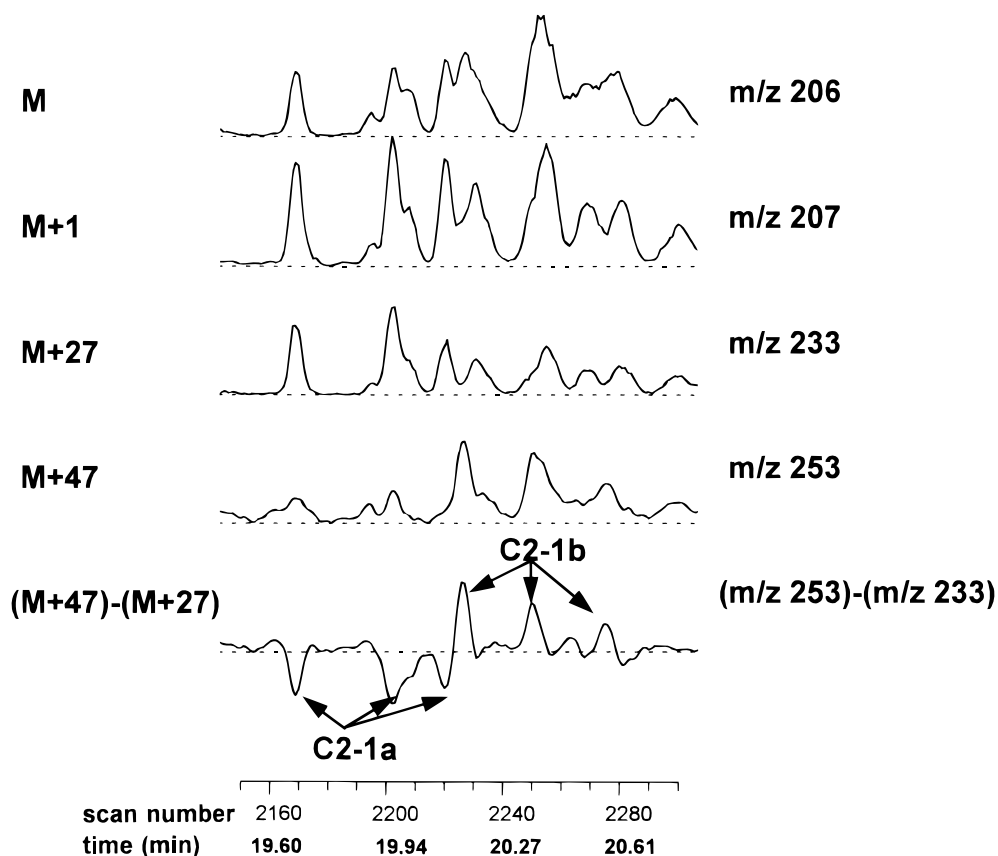


Figure 4. Unsubstituted (C0) phenanthrene/anthracene and fluoranthene/pyrene ion chromatograms from 1,1-DFE CI analysis of sediment extract. Bottom: transformation chromatogram.



**Figure 5.** Monomethyl (C1) phenanthrene/anthracene ion chromatograms and transformation chromatogram from 1,1-DFE CI analysis of sediment extract.



**Figure 6.** Dimethyl/ethyl (C2) phenanthrene/anthracene ion chromatograms and transformation chromatogram from 1,1-DFE CI analysis of sediment extract.

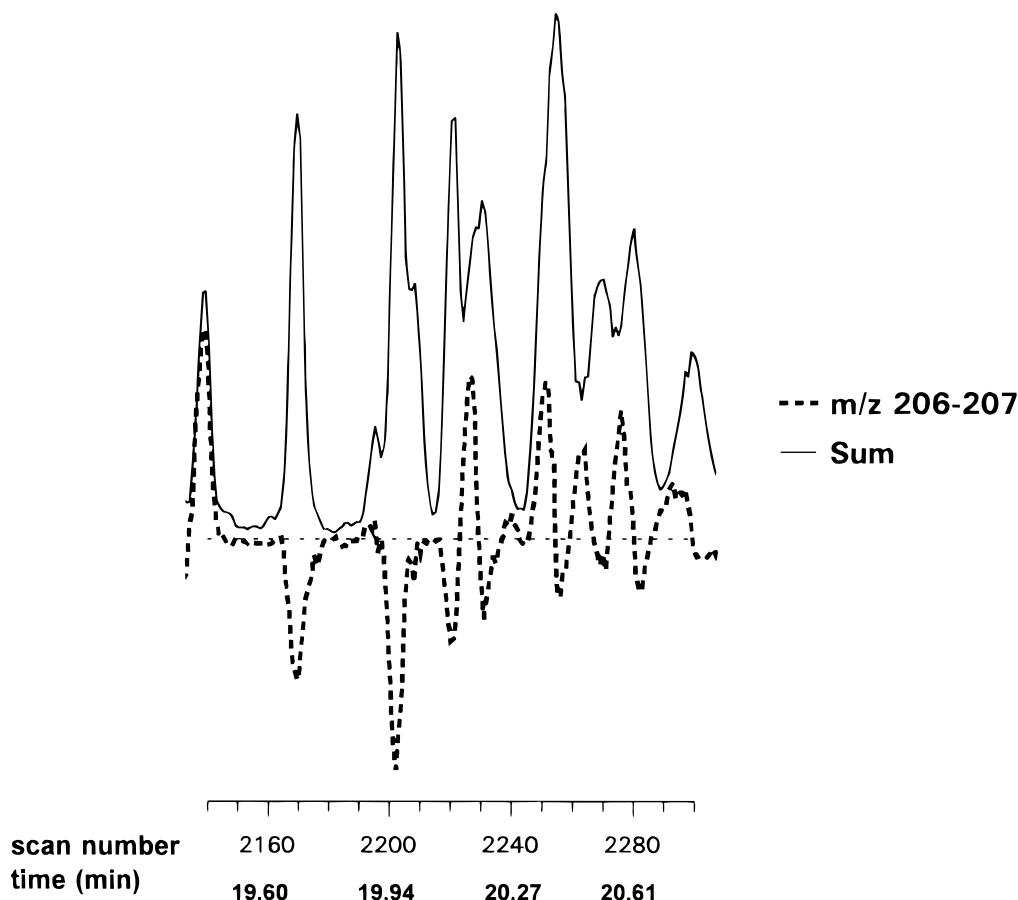


**Figure 7.** Dimethyl/ethyl (C2) phenanthrene/anthracene sum and transformation chromatograms from 1,1-DFE CI analysis of sediment extract.

mass (see Table 1). There are three possible monomethyl isomers for anthracene (1-, 2- and 9-methyl) and five for phenanthrene (1-, 2-, 3-, 4- and 9-methyl). Retention time information from available standards and literature values<sup>7</sup> indicate that 1- and 2-methylantracene co-elute together with 1-, 4- and 9-methylphenanthrenes (scans 2010 to 2050). 9-Methylantracene elutes at a later retention time and is not present in Fig. 5. Under GC/EI-MS conditions it would not be possible to verify the presence of 1- and 2-methylantracene owing to the lack of any characteristic EI ions that would distinguish them from the methylphenanthrenes. However, by generating a characteristic ion ( $m/z$  239) through reaction with  $\text{CH}_3\text{CHF}^+$  ions, the presence of 1- and 2-methylantracene in the sediment extract can be clearly confirmed from the  $m/z$  239 chromatogram (2-methylantracene at scan 2015, 1-methylantracene at scan 2035).

**Mass chromatogram transformations.** As mentioned earlier, transformations can be performed to improve the comparison between mass chromatograms; for this purpose, the chromatograms were normalized prior to subtraction. The results obtained from taking the difference between the normalized  $m/z$  239 and 219 ion chromatograms for the C1 1a/1b data are shown in Fig. 5 (bottom chromatogram). It shows that the methylantracenes plot positive and the methylphenanthrenes negative (with respect to the baseline). The usefulness of

subtracting normalized ion chromatograms for highlighting differences in the elution profile of isomers is further exemplified by the more complex C2 1a/1b homologous series shown in Fig. 6, where the mass chromatograms for the later section of region 1 (Fig. 2) containing C2 analogues of 1a and 1b are displayed. Owing to the larger number of possible isomers in the C2 homologous series, the chromatograms are significantly more complex. Even if a complete set of standards were available, the number of co-eluting species would make differentiation between C2-1b and C2-1a virtually impossible by GC/EI-MS. However, using the mass chromatograms shown in Fig. 6, the presence of both C2 structural isomers groups can be confirmed. Although there are some differences in the elution profiles for C2-1a and C2-1b in the  $m/z$  233 ( $M + 27$ ) and  $m/z$  253 ( $M + 47$ ) ion chromatograms, the normalized transformation chromatogram  $[(M + 47) - (M + 27)]$  ( $m/z$  253–233) clearly shows the  $t_R$  locations for C2-1a (negative plot) and C2-1b (positive plot). Analysis of the mass spectra at scans 2169 and 2227 (Fig. 3) further confirms the presence of C2-1a and C2-1b, respectively.

The chromatogram transformation technique can also be applied to mass chromatograms that display only minor differences, such as the  $M^+$  and  $MH^+$  chromatograms. In fact, it is in these instances when the technique becomes most useful. For example, the results of subtracting the normalized  $m/z$  207 ( $M^+$ ) chromatogram from the normalized  $m/z$  206 ( $MH^+$ ) chromato-



gram are shown in Fig. 7. The  $m/z$  206–207 data (negative plot, C2-1a; positive plot, C2-1b) are plotted together with the normalized sum of the mass chromatograms of the six major ions listed in Table 2 for C2 1a/1b. Similarly to Fig. 6, the presence of the two isomer groups C2-1a and C2-1b is confirmed.

A second transformation which also proved useful, particularly when complex mixtures of isomers are present such as in regions 3 and 4, is  $[(M + 47) - (M + 27)] \times (M + 47)$ . Multiplying the difference chromatogram  $[(M + 47) - (M + 27)]$  by  $(M + 47)$  allows a stronger enhancement of the isomers possessing a large  $(M + 47)$  signal.

To simplify the presentation of the data for regions 2, 3 and 4, in some cases the normalized sum for the six major ions ( $M$ ,  $M + 1$ ,  $M + 27$ ,  $M + 45$ ,  $M + 47$  and  $M + 65$ ) together with the respective transformation chromatograms will be shown only.

### Analysis of isomers in regions 2–4

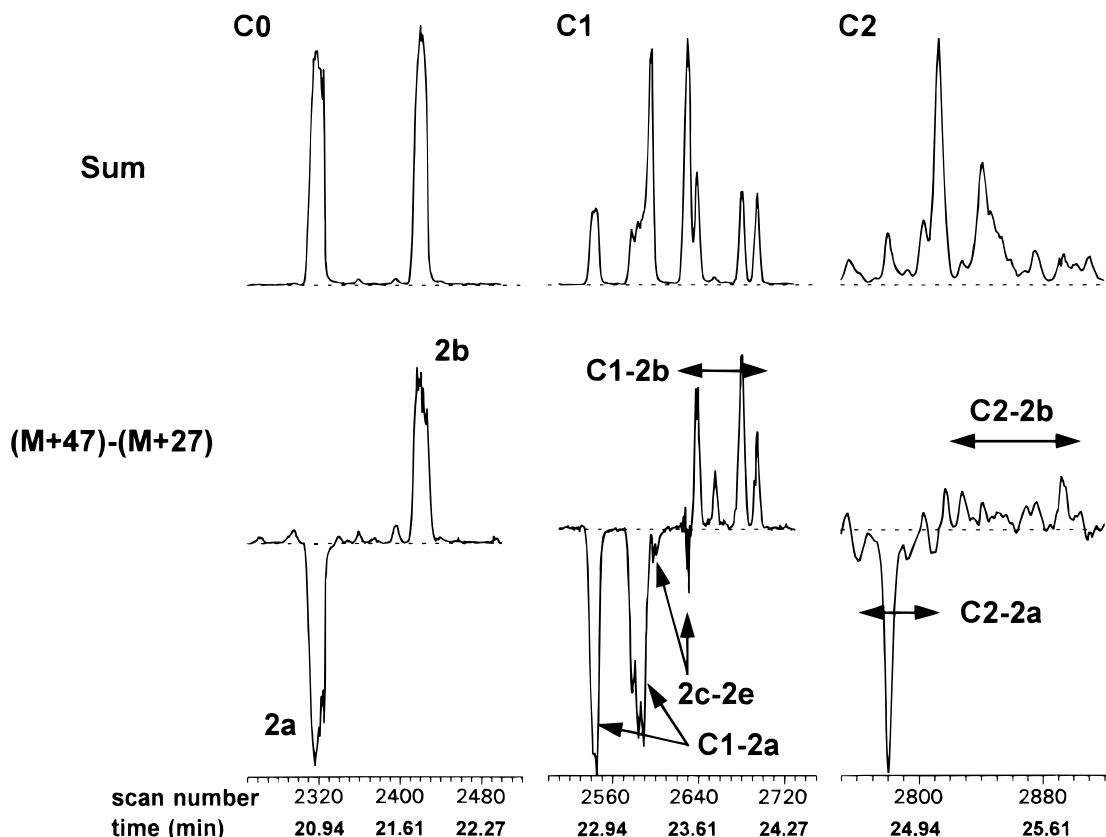
**Region 2.** So far PAHs eluting in region 1 (Fig. 2) have only been discussed. We have found<sup>1</sup> that fluoranthene (2a) and pyrene (2b) compounds eluting in region 2 have adduct-forming behaviour similar to phenanthrene (1a) and anthracene (1b), respectively, as shown in Table 1. Once again it is the alkyl homologous series C1 and C2 which are of interest since the 2a and 2b C0 species are chromatographically well separated. The number of possible monomethyl substitutions on 2a and 2b are five and three, respectively, as indicated by the positions in

Fig. 1. However, another three compounds which co-elute with the C1 2a and 2b species are the benzo[fluorenes (2c, 2d and 2e). They also have a molecular mass of 216 and exhibit EI spectra virtually identical with the C1 2a and 2b species. Fortunately, the adduct mass spectra of these three groups of compounds (C1-2a, C1-2b and 2c–2e) are significantly different (Table 1).

The sum of the normalized extracted ion chromatograms for the six most important ions for the C1 series ( $m/z$  216, 217, 243, 261, 263 and 281) is shown in Fig. 8. 2-Methylfluoranthene (2-MeF) and 2c were identified based on available standards. The remaining compound identifications were made based on mass spectral data and the transformation ion chromatogram  $[(M + 47) - (M + 27)]$  ( $m/z$  263–243). The latter displays the C1-2b compounds as plotting positive and the C1-2a compounds negative. The signals for the 2c–2e compounds are close to zero.

For the C2 series the summed mass chromatogram for  $m/z$  230, 231, 257, 275, 277 and 295 together with the transformation chromatogram are also shown in Fig. 8. The latter clearly shows the deconvolution between the C2-2b (positive plot) and C2-2a compounds (negative plot).

**Region 3.** Isomer analysis becomes more complicated in region 3 owing to the presence of five structural isomers, benzo[*c*]phenanthrene (3a), benz[*a*]anthracene (3b), chrysene (3c), triphenylene (3d) and naphthacene (3e). The identification of these five compounds in the mass chromatogram is shown in Fig. 9(a). A standard was not available for 3a but its retention time relative to



**Figure 8.** Unsubstituted (C0), monomethyl (C1) and dimethyl/ethyl (C2) fluoranthene/pyrene ion and transformation chromatograms from 1,1-DFE CI analysis of sediment extract.

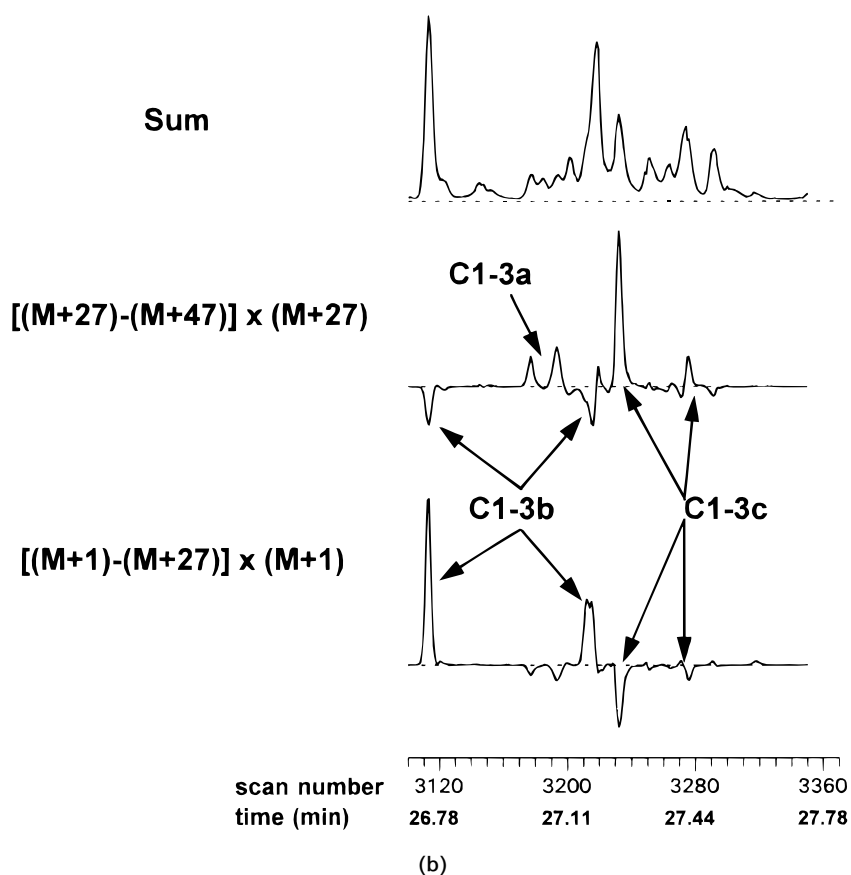
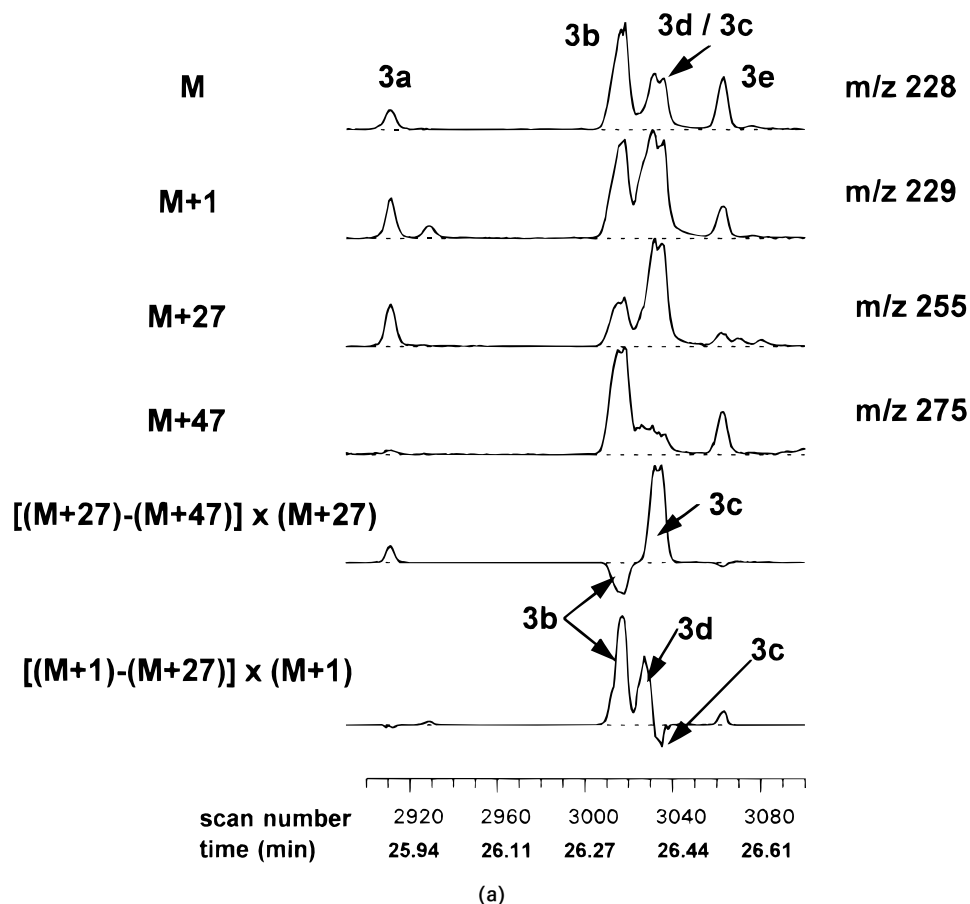
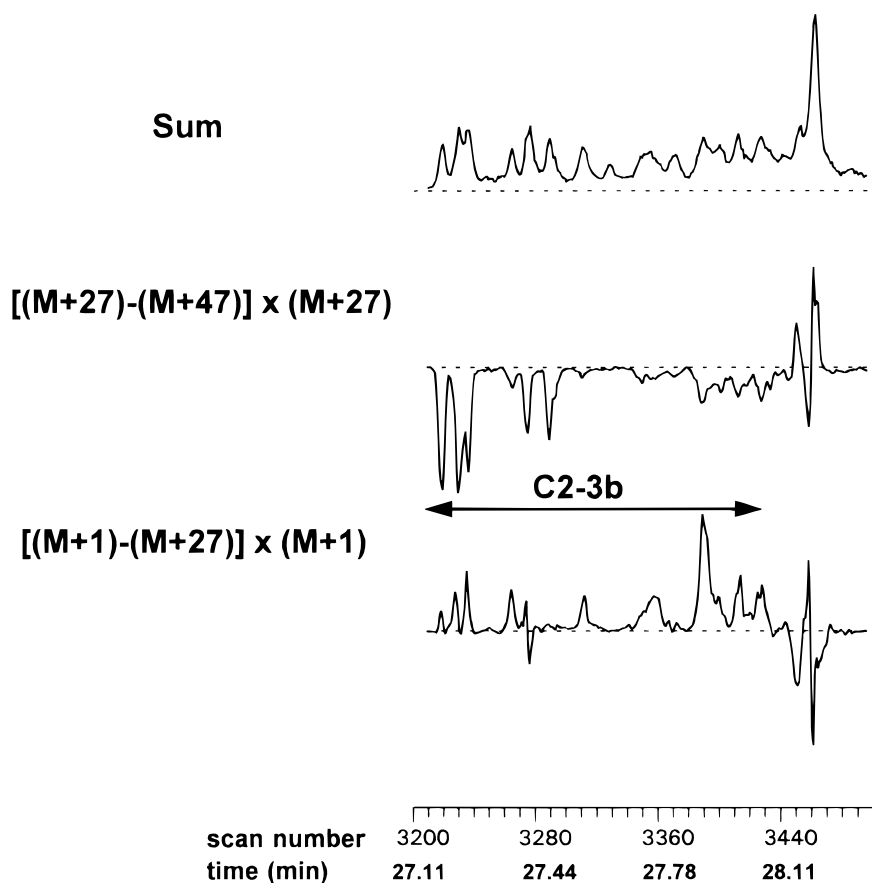


**Figure 9.** Ion and transformation chromatograms for (a) unsubstituted (C0)  $M_r$  228 PAHs, (b) monomethyl (C1)  $M_r$  242 PAHs and (c) dimethyl/ethyl (C2)  $M_r$  256 PAHs.



(c)

Figure 9. Continued

the other four isomers is consistent with literature values.<sup>7</sup> The only co-elution problem in the C0 series is between compounds **3c** and **3d**. The major differences in the mass spectra (Table 1) of these two compounds are the larger amounts of  $m/z$  255 ( $M + 27$ ) formed by **3c** and the larger  $m/z$  229 ( $MH^+$ ) relative abundance for **3d**. With these two trends in mind, the two compounds were partially de-convoluted through  $[(M + 1) - (M + 27)] \times (M + 1)$  transformation in Fig. 9(a). By enhancing the signal for the **3d** characteristic ion ( $m/z$  229) and reducing the signal for the **3c** characteristic ion ( $m/z$  255), this transformation chromatogram produces a positive plot for **3d** and a small negative plot for **3c**. From these data it is possible to observe that **3d** begins to elute just prior to **3c**. This trend can also be observed by comparing the chromatograms of  $m/z$  229 and 255. The former shows a shoulder on the left side of the **3c/3d** peak, corresponding to **3d**, which disappears in the  $m/z$  255 chromatogram.

An  $[(M + 27) - (M + 47)] \times (M + 27)$  transformation was also performed; it enhances the **3c** signal positively and the **3b** signal negatively.

The normalized and summed ( $m/z$  242, 243, 269, 289 and 307) ion chromatogram for the C1 isomers is shown in Fig. 9(b). Compound **3b** has the largest number of possible monomethyl isomers (12; Fig. 1) and would therefore be expected to dominate this series. The second largest C1 isomer group is for **3a** (six isomers) followed by **3c** (four isomers), **3e** (three isomers) and **3d** (two isomers). Using available standards for the

**3a** (2-, 3-, 4- and 5-monomethyl) and **3b** (2-, 4- and 7-monomethyl), it was found that the C1-**3a** series elutes before the C1-**3b** compounds in accordance with the elution order of their unsubstituted analogues in Fig. 9(a).

Analysis of the mass chromatograms, using the same transformations as for C0 data, reveals the presence of a strong positive C1-**3c** signal at scan 3236 resulting from the  $[(M + 27) - (M + 47)] \times (M + 27)$  transformation and a negative signal from transformation  $[(M + 1) - (M + 27)] \times (M + 1)$ , in accordance with the behaviour of **3c** in Fig. 9(a). The other positive signals in the  $[(M + 27) - (M + 47)] \times (M + 27)$  chromatogram are expected to be either C1-**3a** or C1-**3c** as suggested by the data in Fig. 9(a). The two signals between scans 3170 and 3200 are within the elution region expected for C1-**3a** and their mass spectral data confirm the expected high level of  $m/z$  269 (40%) and low levels of the  $m/z$  287, 289, 307 ions (5–10%). The mass spectrum at scan 3275 suggests a C1-**3c** co-eluting with C1-**3b** since the  $m/z$  269 level (20%) is higher than that for pure C1-**3b** but less than that for pure C1-**3c** (C1-**3a** compounds also have high  $m/z$  269 levels but are expected to elute earlier).

The analysis of the C2 data is shown in Fig. 9(c). Using the same set of transformations discussed for the C0 and C1 data, it appears that C2-**3b** compounds dominate this homologous series (negative peaks for  $[(M + 27) - (M + 47)] \times (M + 27)$  and positive peaks for  $[(M + 1) - (M + 27)] \times (M + 1)$ . The remaining

signals in the scan region 3430–3460 correspond to either C2-3a or C2-3c compounds.

**Region 4.** The major C0 structural isomers observed in region 4 are the benzo[*b*]- and -[*k*]fluoranthenes (**4a** and **4b**), benzo[*e*]pyrene (**4c**), benzo[*a*]pyrene (**4d**) and perylene (**4e**). This group of isomers is of both toxicological and environmental interest. Compound **4d** is a potent carcinogen whereas **4c** is not. Compound **4e** is a naturally occurring PAH which can be used as a marker for natural and anthropogenic inputs.<sup>8</sup> Their elution order in the sediment sample is indicated in Fig. 10(a) according to their mass spectral data and retention times of standards. With the exception of **4a** and **4b**, these compounds are well resolved. However, as expected, the same is not true for the C1 isomers, as shown in the normalized summed (*m/z* 266, 267, 293, 311, 313, 331) chromatogram in Fig. 10(b). Fortunately, these compounds have significantly different adduct-forming behaviour.

Transformations performed on the two sets of mass chromatograms displaying the largest differences are shown in Fig. 10(a). Transformation  $[(M + 47) - (M + 27)] \times (M + 47)$  enables **4a** and **4b** to plot negative while enhancing **4c** over **4d** and **4e**. Conversely, transformation  $[M - (M + 27)] \times M$  strongly enhances the **4d** signal. When the same set of transformations was applied to the C1 data [Fig. 10(b)] a remarkable deconvolution resulted when compared

with the normalized summed mass chromatogram. The  $[(M + 47) - (M + 27)] \times (M + 47)$  transformation clearly shows the C1-**4a** and -**4b** isomers (negative plots) and C1-**4c** isomers (enhanced positive plots). The second transformation  $[M - (M + 27)] \times M$  shows the C1-**4d** isomers enhanced positively whereas the C1-**4c** isomers from the previous chromatogram have disappeared. Further confirmation of the elution of the C1-**4d** isomers in this region was obtained from three available standards (8-, 9- and 10-monomethyl-**4d**). The elution of C1-**4e** isomers can be assigned to the signals between 3860 and 3900 in the lower chromatogram in Fig. 10(b), since these signals are not present in the  $[(M + 47) - (M + 27)] \times (M + 47)$  transformation, in accordance with C0-**4e** in the same transformation in Fig. 10(a).

### Quantitation

As demonstrated previously,<sup>1</sup> under ARC conditions the effect of concentration does not alter the adduct-forming behaviour of isomers over a concentration range of at least three orders of magnitude. Analysis of the 1,1-DFE adducts from a dilution series of 16 PAH standards displayed a log-log linear dynamic range from 50 to 28 000 pg, similar to EI data for the same compounds based on the calibration curve data (log

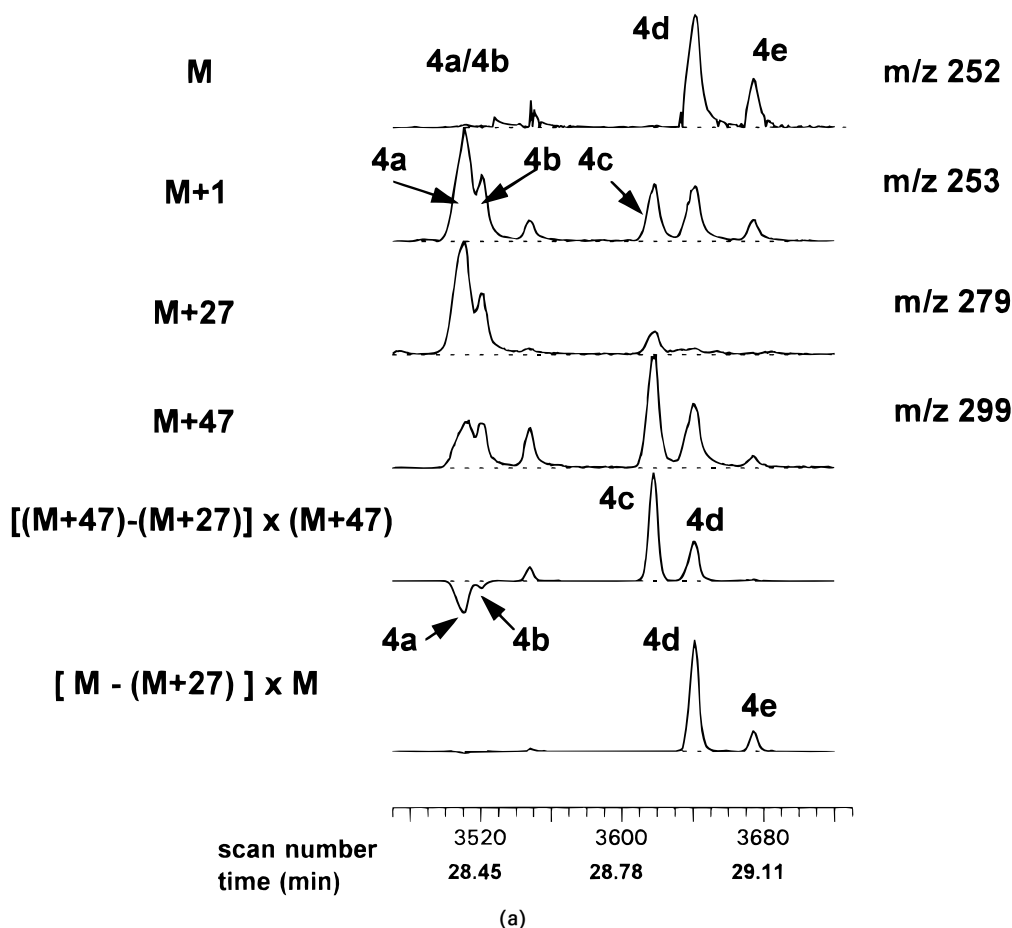


**Figure 10.** Ion and transformation chromatograms for (a) unsubstituted (C0) M, 252 PAHs and (b) monomethyl (C1) M, 266 PAHs.

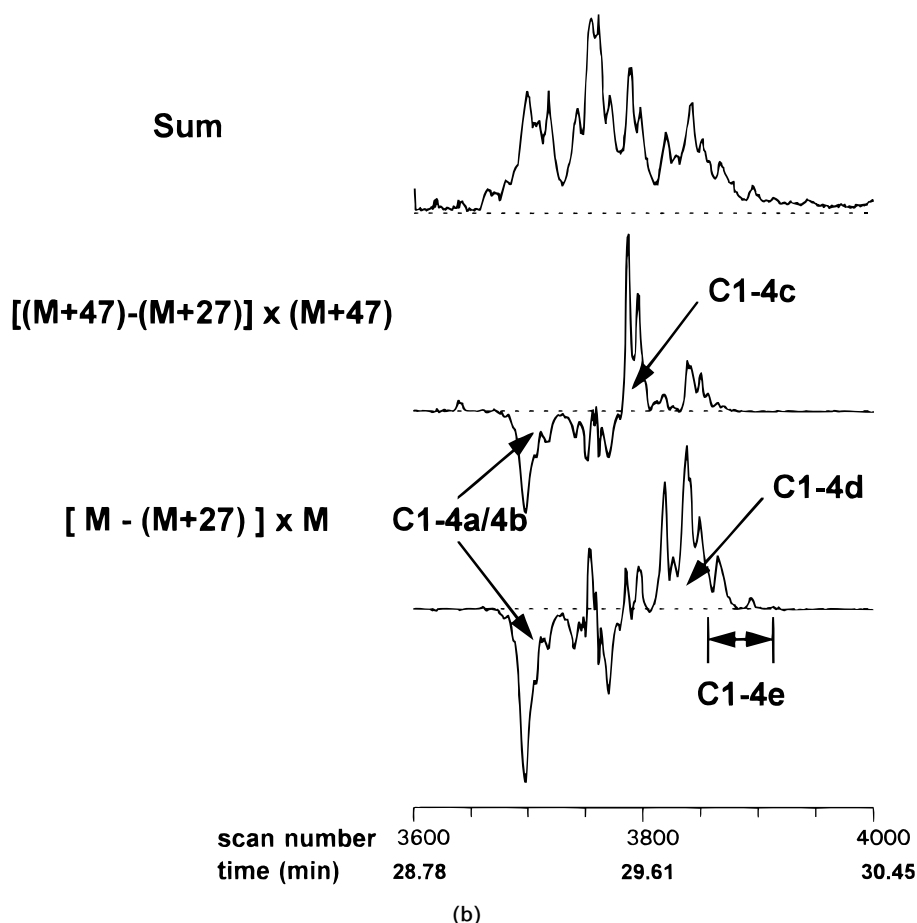


Figure 10. Continued

area vs log pg data: EI  $m/z$  202 **2a**, slope = 1.17, intercept = 1.48,  $r = 1.000$ ; CI  $m/z$  202 **2a**, slope = 1.05, intercept = 0.70,  $r = 0.999$ ; CI  $m/z$  229 **2a**, slope = 0.866, intercept = 1.44,  $r = 0.998$ . For the EI data the  $m/z$  202 ion displays only a marginally better correlation coefficient ( $r$ ) and a slightly higher slope, signifying a slightly better calibration sensitivity. The  $m/z$  229 ( $M + 27$ ) adduct ion also shows a good linear fit, indicating that these species are also analytically reliable. The limits of detection (LOD) for PAHs in the sediment extract were calculated using the equation [1] where  $m$  is the slope of the calibration curve (or response factor area/quantity) at the low concentration limit and  $A_n$  is the integrated area of the noise above the baseline.

$$\text{LOD} = \frac{3A_n}{m} \quad (1)$$

Using the  $m/z$  202 CI data for **2a**, LOD values of 170 pg in the sediment extract ( $A_n = 500$ ,  $m = 9 \text{ pg}^{-1}$ ) and 50 pg ( $A_n = 150$ ,  $m = 9 \text{ pg}^{-1}$ ) in a standard solution were obtained.

The presence of multiple adduct ions for most isomers in this study provides a wide choice for quantitation. Generally one selects the most abundant ion; however, when co-eluting compounds have to be quantified the best choice will be ions that are characteristic of each compound. For example, for a C1 **1a/1b** mixture, using the  $m/z$  239 and ions should offer the

best results (Table 1). As reported previously,<sup>1</sup> the relative compound proportions for a pair of co-eluting isomers can be determined from the ratio of adduct ions formed.

## CONCLUSION

Differentiation of PAH isomers in environmental extracts containing multiple co-eluting or overlapping compounds is not a trivial task. Using 1,1-DFE as a CI reagent it has been demonstrated that the formation of adduct ions with PAHs permits differentiation between the isomers. Through the use of ion chromatogram analysis and transformations, a number of PAH isomer groups, present in a contaminated sediment extract, could be deconvoluted. To the best of our knowledge, this is the first time that deconvolution of PAH isomer data from a real environmental sample has been reported.

## Acknowledgements

The authors thank Varian Canada for the extended loan of the MS/MS and CI features of the Saturn 4D ion trap. They acknowledge financial support from Dr K. Reimer of the Royal Canadian Military College Environmental Sciences Group, from the Department of Indian and Northern Development (DIAND) and from the National Science and Engineering Research Council of Canada.

## REFERENCES

1. A. A. Mosi, W. R. Cullen and G. K. Eigendorf, *J. Mass Spectrom.* **32**, 864 (1997).
2. *Polycyclic Aromatic Hydrocarbons in the Aquatic Environment: Formation, Sources, Fate and Effects on Aquatic Systems*. NRCC Publication No. NRCC 18981, NRCC, Ottawa (1983).
3. R. G. Harvey, *Polycyclic Hydrocarbons and Carcinogens*. ACS Symposium Series, No. 283. American Chemical Society, Washington, DC (1985).
4. M. B. Yunker, R. W. MacDonald, W. J. Cretney, B. R. Fowler and F. A. McLaughlin, *Geochim. Cosmochim. Acta* **57**, 3041 (1993).
5. R. Roussel, M. Allaire and R. S. Friar, *J. Air Waste Manage. Assoc.* **42**, 1609 (1992).
6. C. D. Simpson, A. A. Mosi, W. R. Cullen and K. J. Reimer, *Sci. Total Environ.* **181**, 265 (1996).
7. G. Grimmer, J. Jacob, G. Dettbarn and K.-W. Naujack, *Fresenius' Z. Anal. Chem.* **322**, 595 (1985).
8. M. I. Venkatesan, *Mar. Chem.* **25**, 1 (1988).